

# Emergence of warm inflation in curved space-time between accelerating branes

Aroonkumar Beesham\*

*Department of Mathematical Sciences, University of Zululand,*

*Private Bag X1001, Kwa-Dlangezwa 3886, South Africa*

It appears that having our own brane to somehow interact with other branes could give rise to quite an interesting system and that that interaction could lead to some observable effects. We consider the question of whether or not these signatures of interaction between the branes can be observed. To answer this question, we investigate the effect induced by the inflaton in the WMAP7 data using the warm inflationary model. In this model, slow-roll and perturbation parameters are given in terms of the inflaton thermal distribution. We show that this distribution depends on the orbital radius of the brane motion under the interaction potential of other branes in extra dimensions. Thus, an enhancement in the brane inflation can be a signature of an orbital motion in extra dimensions and consequently, some signals of other branes can be detected by observational data. According to experimental data, the  $N \simeq 50$  case leads to  $n_s \simeq 0.96$ , where  $N$  and  $n_s$  are the number of e-folds and the spectral index, respectively. This standard case may be found in the range  $0.01 < R_{Tensor-scalar} < 0.22$ , where  $R_{Tensor-scalar}$  is the tensor-scalar ratio. We find that at this point, the radial distance between our brane and another brane is  $R = (1.5GeV)^{-1}$  in intermediate, and  $R = (0.02225GeV)^{-1}$  in logamediate inflation.

## I. INTRODUCTION

Recently, it was argued that the boundary conditions to be imposed on the quantum state of the whole multiverse could be such that brane universes could be created in entangled pairs [1]. Also, the consideration of entanglement between the quantum states of two or more brane universes in a multiverse scenario provides us with a completely new paradigm that

---

\* abeesham@yahoo.com

opens the door to novel approaches for traditionally unsolved problems in cosmology, more precisely, the problems of the cosmological constant, the arrow of time and the choice of boundary conditions, amongst others [2]. Some authors have tried to find direct evidence of the existence of other brane universes using a dark energy model [3]. Also some researchers show that other branes are made observable for us through interaction with our own brane [4]. In their paper, the orbital radius of our brane in extra dimensions can be described according to the interaction potential of other branes. In some scenarios, the properties of the interaction potential are calculated for a composite quantum state of two branes whose states are quantum mechanically correlated [1, 2]. It appears that having our own brane to somehow interact with other branes could give rise to quite an interesting system, and that that interaction could lead to an orbital motion in extra dimensions.

The main question is the possibility of considering the properties of other branes against observational data? The warm inflationary model helps us to perform precision tests of the universal extra dimensional models, and explore the new physics against observational data. In this scenario, after the period of inflation, the radiation of the universe becomes dominant and the reheating epoch will not happen. The results of this model are compatible with WMAP7 and Planck data [5]. In this theory, slow-roll and perturbation parameters are given in terms of the thermal distribution of the inflaton. On the other hand, this distribution is given in terms of the orbital radius of the brane motion [4] in extra dimensions. As the interaction potential increases, the effect of the inflaton radiation from the horizon that appears in the brane-antibrane system on the universe's inflation becomes systematically more effective because at higher energies, there exist more channels for inflaton production and its decay into particles.

The outline of the paper is as the following. In section II, we consider the effect of the orbital radius of the brane motion under the interaction potential of the other branes on the thermal distribution of inflatons. In section III, using the warm inflationary model, we analyze the signature of other branes against observational data. The last section is devoted to a summary and conclusion.

## II. THE THERMAL DISTRIBUTION OF INFLATONS NEAR THE APPEARED HORIZON IN THE BRANE-ANTIBRANE SYSTEM

Previously, the dynamical behavior of a pair of Dp and anti Dp branes which move parallel to each other in the region that the brane and antibrane annihilation will not occur was considered [4]. Also, the orbital radius of the brane motion due to the interaction potential in extra dimensions was studied. Using these results, we calculate the thermal distribution of inflatons near the horizon that appears in the brane-antibrane system and show that the thermal distribution of inflatons can be given in terms of the orbital radius of the brane motion in extra dimensions.

The d-dimensional metric in the brane-antibrane system is expressed as:

$$ds^2 = g_{\mu\nu}dx^\mu dx^\nu + g_{\rho\sigma}dx^\rho dx^\sigma + g_{ab}dx^a dx^b \quad (1)$$

where  $g_{\mu\nu}$  and  $g_{\rho\sigma}$  are the p-dimensional metrics along the Dp and the anti Dp brane, respectively, and  $g_{ab}$  is the (d-2p) dimensional metric along the transverse coordinates.

Now let us consider the wave equation of the inflaton in extra dimensions between two branes:

$$\left\{ -\frac{\partial^2}{c^2 \partial \chi^2} + \frac{\partial^2}{\partial r^2} \right\} B = 0 \quad (2)$$

where  $\chi, r$  are the transverse coordinates between the two branes. This equation corresponds to flat space-time. The interaction potential between the Dp brane-anti Dp brane in extra dimensions is of the type [4]

$$V(R) \sim \frac{64\pi^2 \mu^4}{27} \quad (3)$$

where  $\mu^4 = \frac{27}{32\pi^2} T_3 h^4$ ,  $h(R) = \frac{b^4}{R^4}$ ,  $R$  is the orbital radius distance between the two branes,  $T_3$  the brane tension and  $b$  the curvature radius of the  $AdS_5$  throat. This potential leads to curved space-time.

Thus, to write the inflaton wave equation in curved space-time, we should use the following reparameterizations:

$$\begin{aligned} r &\rightarrow \rho(r, \chi) \\ \chi &\rightarrow \tau(r, \chi) \end{aligned} \quad (4)$$

that leads to the following inflaton wave equation:

$$\left[ \left\{ \left( \frac{\partial \tau}{\partial r} \right)^2 - \left( \frac{\partial \tau}{\partial \chi} \right)^2 \right\} \frac{\partial^2}{c^2 \partial \tau^2} + \left\{ \left( \frac{\partial \rho}{\partial r} \right)^2 - \left( \frac{\partial \rho}{\partial \chi} \right)^2 \right\} \frac{\partial^2}{\partial \rho^2} \right] B = 0 \quad (5)$$

We can normalize the distance between the two branes to unity by making the following choices:

$$\begin{aligned} \rho(r, \chi) &= \frac{r}{R(\chi)} \\ \tau &= \beta c^2 \int_0^\chi dt \frac{R(\dot{\chi})}{\dot{R}(\dot{\chi})} - \beta \frac{r^2}{2} \end{aligned} \quad (6)$$

With the above considerations, the wave equation is written as:

$$(-g)^{1/2} \frac{\partial}{\partial x^\mu} [g^{\mu\nu} (-g)^{1/2} \frac{\partial}{\partial x^\nu}] B = 0 \quad (7)$$

where  $x^5 = \tau$ ,  $x^4 = \rho$  and the metric elements are obtained as:

$$\begin{aligned} g^{\tau\tau} &= -\frac{1}{\beta^2 c^2} \left( \frac{R}{\dot{R}} \right) \left( \frac{1 - \frac{\dot{R}^2}{c^2} \rho^2}{1 + \frac{\dot{R}^2}{c^2} \rho^2} \right) \\ g^{44} &= R^2 \left( \frac{1 + \frac{\dot{R}^2}{c^2} \rho^2}{1 - \frac{\dot{R}^2}{c^2} \rho^2} \right) \end{aligned} \quad (8)$$

The horizon of this system is located at:

$$r_{horizon} = \frac{cR}{\dot{R}} \quad (9)$$

where  $c$  is velocity of light. In Kruskal coordinates the metric of system becomes [6, 7]:

$$\begin{aligned} ds^2 &= g_{\mu\nu} dx^\mu dx^\nu + g_{\rho\sigma} dx^\rho dx^\sigma - r_{horizon} \frac{e^{-\frac{r}{r_{horizon}}}}{r} d\bar{u} d\bar{v} + r^2 d\theta^2 \\ \bar{u} &= -2r_{horizon} e^{-u/2r_{horizon}}, \bar{v} = -2r_{horizon} e^{-v/2r_{horizon}} \\ u &= \chi - r^*, v = \chi + r^*, r^* = -r - r_{horizon} \ln |r - r_{horizon}| \end{aligned} \quad (10)$$

Since the Killing vector in Kruskal coordinates is given by  $\frac{\partial}{\partial \bar{u}}$  on the past horizon  $H^-$ , the positive frequency normal mode solution in Kruskal coordinates is approximated by:

$$B \propto e^{-i\omega \bar{u}} \quad (11)$$

where  $\omega$  is the inflaton energy in extra dimensions. Using this fact that  $\bar{v} = 0$  on  $H^-$  [7] we can estimate the original positive frequency normal mode on the past horizon as:

$$B \propto e^{-i\omega u} = \left(\frac{|\bar{u}|}{2r_{horizon}}\right)^{-i2r_{horizon}\omega} = \begin{cases} \left(-\frac{\bar{u}}{2r_{horizon}}\right)^{-i2r_{horizon}\omega} & (region I) \\ \left(\frac{\bar{u}}{2r_{horizon}}\right)^{-i2r_{horizon}r_{horizon}} & (region II) \end{cases} \quad (12)$$

In Eq. (12), we can use the fact that  $(-1)^{-i2r_{horizon}\omega} = e^{2r_{horizon}\omega}$ . Using equation (12) we observe that the inflaton states in the horizon satisfy the following condition [7, 8]:

$$\begin{aligned} (B_{out} - \tanh r_\omega B_{in})|system\rangle_{in} \otimes_{out} &= 0 \\ \tanh r_\omega &= e^{-2r_{horizon}\omega} \end{aligned} \quad (13)$$

which actually constitutes a boundary state. In fact, we can view Hawking radiation as the pair creation of a positive energy field that goes to infinity and a negative energy field that falls into the horizon of the brane-antibrane system. The pair is created in a particular entangled state. So the Unruh state can be viewed as an entangled thermal state. The above definition of the positive frequency solution in terms of  $B_{out}$  and  $B_{in}$  leads to the Bogoliubov transformation [6–8] for the particle creation and annihilation operators in the brane-antibrane system and Minkowski space-times in the exterior region of the system:

$$\begin{aligned} d &= \cosh r_\omega \alpha_{out} - \sinh r_\omega \alpha_{in}^\dagger \\ d^\dagger &= \cosh r_\omega \alpha_{out}^\dagger - \sinh r_\omega \alpha_{in} \\ \tanh r_\omega &= e^{-2\pi r_{horizon}\omega} \end{aligned} \quad (14)$$

where  $d^\dagger$  and  $d$  are the creation and annihilation operators, respectively, acting on the Minkowski vacuum,  $\alpha_{out}^\dagger$  and  $\alpha_{out}$  the respective operators acting on the brane-antibrane vacuum outside the event horizon, and  $\alpha_{in}^\dagger$  and  $\alpha_{in}$  are the respective operators acting on the brane-antibrane vacuum inside the event horizon.

Thus, we can write the Bogoliubov transformation between the Minkowski and curved creation and annihilation operators as:

$$d|system\rangle_{out} \otimes_{in} = (\alpha_{out} - \tanh r_\omega \alpha_{in}^\dagger)|system\rangle_{out} \otimes_{in} = 0 \quad (15)$$

which actually constitutes a boundary state. Now, we assume that the system vacuum  $|system\rangle_{out} \otimes_{in}$  is related to the flat vacuum  $|0\rangle_{flat}$  by

$$|system\rangle_{out} \otimes_{in} = F|0\rangle_{flat} \quad (16)$$

where  $F$  is a function to be determined later.

From  $[\alpha_{out}, \alpha_{out}^\dagger] = 1$ , we obtain  $[\alpha_{out}, (\alpha_{out}^\dagger)^m] = \frac{\partial}{\partial \alpha_{out}^\dagger} (\alpha_{out}^\dagger)^m$  and  $[\alpha_{out}, F] = \frac{\partial}{\partial \alpha_{out}^\dagger} F$ . Then using Eqs.(15) and (16), we get the following differential equations for  $F$ :

$$\left(\frac{\partial F}{\partial \alpha_{out}^\dagger} - \tanh r_\omega \alpha_{in}^\dagger F\right) = 0 \quad (17)$$

and the solution is given by

$$F = e^{\tanh r_\omega \alpha_{out}^\dagger \alpha_{in}^\dagger} \quad (18)$$

By substituting Eq. (18) into Eq. (16) and by properly normalizing the state vector, we get

$$\begin{aligned} |\text{system}\rangle_{out} \otimes_{in} &= N e^{\tanh r_\omega \alpha_{in}^\dagger \alpha_{out}^\dagger} |0\rangle_{flat} \\ &= \frac{1}{\cosh r_\omega} \sum_m \tanh^m r_\omega |m\rangle_{out} \otimes |\bar{m}\rangle_{in} \end{aligned} \quad (19)$$

where  $|m\rangle_{in}$  and  $|\bar{m}\rangle_{out}$  are the orthonormal bases (normal mode solutions) for a particle that acts on  $H_{in}$  and  $H_{out}$  respectively, and  $N$  is the normalization constant.

Eq. (19) expresses that the states inside and outside the horizon are entangled. However, this entanglement depends on the event horizon and the horizon is given in terms of  $R$ , the orbital radius of the brane motion in the interaction potential of the other brane,  $r_{horizon} = \frac{cR}{R}$ , and consequently, the entanglement changes with the orbital radial distance between the two branes. We derive the thermal distribution for inflatons in extra dimensions as the following:

$$\begin{aligned} \langle B \rangle_{out \otimes in} &= \langle \text{system} | \alpha_{in}^\dagger \alpha_{in} | \text{system} \rangle_{out \otimes in} \\ &= \frac{e^{-2\pi r_{horizon} \omega}}{1 - e^{-2\pi r_{horizon} \omega}} \end{aligned} \quad (20)$$

The above equation shows that different numbers of inflatons are produced with different probabilities inside and outside of the apparent horizon in the brane-antibrane system. These probabilities are related to the orbital radial distance of the two branes and the energy of the inflatons.

### III. CONSIDERING THE EFFECT OF OTHER BRANES ON COSMIC INFLATION BY USING WARM INFLATIONARY MODEL

In this section we enter the effects of the interaction potential between the branes on the results of the derivation of slow-roll, perturbation parameters and other important parameters in the inflationary model [5]. We show that these parameters are given in terms of

the orbital radial distance between the two branes and describe the shape of the interaction potential between branes. Also, using the inflationary model, we discuss the signature of interaction between branes against observational data.

Previously, it has been shown that in the FRW brane with the metric

$$ds^2 = g_{\mu\nu} dx^\mu dx^\nu = -dt^2 - a^2(t) dx^i dx_i \quad (21)$$

the dynamics of warm inflation is presented by these equations [5]:

$$\begin{aligned} \dot{\rho} + 3H(P + \rho) &= -\Gamma \langle \dot{B} \rangle^2 \\ \dot{\rho}_\gamma + 4H\rho_\gamma &= -\Gamma \langle \dot{B} \rangle^2 \\ H^2 &= \frac{1}{2}(\langle \dot{B} \rangle^2 + V(B)) + \frac{1}{3}\rho_\gamma \\ V(B) &= m^2 \langle B \rangle^2 \end{aligned} \quad (22)$$

where  $\rho$  is the energy density,  $p$  the pressure,  $\rho_\gamma$  the energy density of the radiation,  $\Gamma$  the dissipative coefficient,  $\langle B \rangle$  the thermal distribution of the inflaton, and the overdot ( $\dot{\phantom{x}}$ ) is the derivative with respect to cosmic time. In the previous section, we discussed that the thermal distribution of the inflaton can be given as a function of the orbital radial distance between branes. Using this fact, we can rewrite the above equation as:

$$\begin{aligned} \dot{\rho} + 3H(P + \rho) &= -\Gamma \left( \frac{\ddot{R}R - \dot{R}^2}{2\pi\omega R^2} \right)^2 \\ \dot{\rho}_\gamma + 4H\rho_\gamma &= -\Gamma \left( \frac{\ddot{R}R - \dot{R}^2}{2\pi\omega R^2} \right)^2 \\ H^2 &= \frac{1}{2} \left( \left( \frac{\ddot{R}R - \dot{R}^2}{2\pi\omega R^2} \right)^2 + V(R, \dot{R}) \right) + \frac{1}{3}\rho_\gamma \\ V(R, \dot{R}) &= m^2 \left( 1 - \frac{\dot{R}}{2\pi\omega R} \right)^2 \end{aligned} \quad (23)$$

Using quantum field theory methods [9, 10], the dissipation coefficient ( $\Gamma$ ) in the above equations could be calculated as:

$$\Gamma = \Gamma_0 \frac{T^3}{\langle B \rangle^2} \sim \Gamma_0 \frac{4\pi^2 \omega^2 T^3 R^2}{\dot{R}^2} \quad (24)$$

where  $T$  is the temperature of the thermal bath. During the inflationary epoch, the energy density  $\rho$  is more than the radiation energy density  $\rho > \rho_\gamma$ ; however, it is comparable with the potential energy density  $V(B^2)$  ( $\rho \sim V$ ) [5]. The slow-roll approximation ( $\langle \ddot{B} \rangle \leq$

$(3H + \frac{\Gamma}{3}) < \dot{B} >$  [11] with the condition that inflation radiation production be quasi-stable,  $(\dot{\rho}_\gamma \leq 4H\rho_\gamma, \dot{\rho}_\gamma \leq \Gamma < \dot{B} >)$  leads to following dynamic equations [5]

$$\begin{aligned} 3H(1 + \frac{r}{3}) < \dot{B} > &= -\frac{1}{2}\dot{V} \\ \rho_\gamma &= \frac{3}{4}r < \dot{B} >^2 = \frac{r}{(1 + \frac{r}{3})^2} \frac{\dot{V}^2}{V} = CT^4 \\ H^2 &= \frac{1}{2}V \end{aligned} \quad (25)$$

where  $r = \frac{\Gamma}{3H}$ , and  $C = \frac{\pi^2 g^*}{30}$  ( $g^*$  are the number of relativistic degrees of freedom). In the above equations, a prime ( $\dot{\phantom{x}}$ ) denotes a derivative with respect to the field  $\mathbf{B}$ . Using this equation and the thermal distribution of the inflaton in Eq. (20), we can obtain the dynamic equations with respect to  $R$ , the orbital radial distance between the two branes:

$$\begin{aligned} 3H(1 + \frac{r}{3}) \left( \frac{\ddot{R}R - \dot{R}^2}{2\pi\omega R^2} \right) &= -\frac{1}{2}\dot{V}(R, \dot{R}) \\ \rho_\gamma &= \frac{3}{4}r \left( \frac{\ddot{R}R - \dot{R}^2}{2\pi\omega R^2} \right)^2 = \frac{r}{(1 + \frac{r}{3})^2} \frac{\dot{V}^2(R, \dot{R})}{V(R, \dot{R})} = CT^4 \\ H^2 &= \frac{1}{2}V(R, \dot{R}) \end{aligned} \quad (26)$$

where the prime ( $\dot{\phantom{x}}$ ) denotes derivative with respect to  $R$ . From the above equations, the temperature of the thermal bath is given by[5]:

$$T = \left[ -\frac{r\dot{H}}{2C(1 + \frac{r}{3})} \right]^{\frac{1}{4}} = \left[ -\frac{r(\ddot{R}R - \dot{R}^2)}{4C\pi\omega R^2(1 + \frac{r}{3})} \right]^{\frac{1}{4}} \quad (27)$$

This temperature depends on the orbital radial distance between the two branes. As the branes come close to each other, the temperature of the thermal bath increases. The reason for this is as follows: with decreasing distance between the two branes, the interaction potential increases and more inflatons radiate from the apparent horizon of the brane-antibrane system.

At this stage, we tend to calculate the dependency of slow-roll parameters on the orbital radial distance between different branes. These parameters in warm inflation are [5]:

$$\begin{aligned} \epsilon &= -\frac{1}{H} \frac{d}{dt} \ln(H) \\ \eta &= -\frac{\ddot{H}}{H\dot{H}} \end{aligned} \quad (28)$$

where  $H = \frac{\dot{a}}{a}$  and  $a$  is the scale factor. To calculate these parameters, we should determine the explicit form of the scale factor.



Until now, eight possible asymptotic solutions for cosmological dynamics have been proposed [12]. Three of these solutions have non-inflationary scale factor and another three solutions give de Sitter, intermediate and power-low inflationary expansion. Finally, two cases of these solutions have asymptotic expansion with scale factor ( $a = a_0 \exp(A(\ln t)^\lambda)$ ). This version of inflation is named logamediate inflation [13]. In this paper, we will study the warm-tachyon inflationary model in the scenarios of intermediate and logamediate inflation.

Firstly, let us consider intermediate inflationary expansion. In this model, the expansion of the universe is between standard de Sitter inflation with scale factor  $a(t) = a_0 \exp(H_0 t)$  and power law inflation with scale factor  $a(t) = t^p, p > 1$  (slower than the first one) [14, 15]. The scale factor of this model has the form below [16, 17]:

$$a = a_0 \exp(At^f), 0 < f < 1 \quad (29)$$

where  $A$  is a positive constant. The number of e-folds in this case is [5]:

$$N = \int_{t_1}^t H dt = A(t^f - t_1^f) \quad (30)$$

where  $t_1$  is the beginning time of inflation. From Eqs.(20), (24), (25), (26), (27) and (29) we obtain the Hubble parameter as:

$$\begin{aligned} H &= fA \left( \frac{\ln \langle B \rangle - \ln \langle B_0 \rangle}{\bar{\omega}} \right)^{\frac{8(f-1)}{5f+2}} = \\ &fA \left( \frac{\ln \frac{e^{-2\pi r_{horizon}\omega}}{1-e^{-2\pi r_{horizon}\omega}} - \ln \frac{e^{-2\pi r_{0,horizon}\omega}}{1-e^{-2\pi r_{0,horizon}\omega}}}{\bar{\omega}} \right)^{\frac{8(f-1)}{5f+2}} \sim \\ &fA \left( \frac{-2\pi\omega(r_{horizon} - r_{0,horizon}) + \ln \frac{1-e^{-2\pi r_{0,horizon}\omega}}{1-e^{-2\pi r_{horizon}\omega}}}{\bar{\omega}} \right)^{\frac{8(f-1)}{5f+2}} \sim \\ &fA \left( \frac{2\pi\omega \left( \frac{R_0}{R_0} - \frac{R}{R} \right) + \ln \frac{1-e^{-2\pi \frac{R_0}{R_0}\omega}}{1-e^{-2\pi \frac{R}{R}\omega}}}{\bar{\omega}} \right)^{\frac{8(f-1)}{5f+2}} \\ B &= B_0 \exp(\bar{\omega} t^{\frac{5f+2}{8}}) \end{aligned} \quad (31)$$

where  $\bar{\omega} = \left( \frac{6}{\Gamma_0} \left( \frac{2C}{3} \right)^{\frac{3}{4}} \right)^{\frac{1}{2}} \left( \frac{8(fA)^{\frac{5}{8}} (1-f)^{\frac{1}{8}}}{5f+2} \right)$  and  $\Gamma_0 = constant$ . This equation insists that the evolution of our brane universe is affected by the number of inflatons that are radiated from the apparent horizon of the brane-antibrane system and it changes with an increase or decrease in the orbital radial distance between the two branes.

The important slow-roll parameters  $\epsilon$  and  $\eta$  are given by:

$$\epsilon = \frac{1-f}{fA} \left( \frac{\ln \langle B \rangle - \ln \langle B_0 \rangle}{\bar{\omega}} \right)^{-\frac{8f}{5f+2}} =$$

$$\begin{aligned}
& \frac{1-f}{fA} \left( \frac{\ln \frac{e^{-2\pi r_{horizon}\omega}}{1-e^{-2\pi r_{horizon}\omega}} - \ln \frac{e^{-2\pi r_{0,horizon}\omega}}{1-e^{-2\pi r_{0,horizon}\omega}}}{\bar{\omega}} \right)^{-\frac{8f}{5f+2}} \sim \\
& \frac{1-f}{fA} \left( \frac{-2\pi\omega(r_{horizon} - r_{0,horizon}) + \ln \frac{1-e^{-2\pi r_{0,horizon}\omega}}{1-e^{-2\pi r_{horizon}\omega}}}{\bar{\omega}} \right)^{-\frac{8f}{5f+2}} \sim \\
& \frac{1-f}{fA} \left( \frac{2\pi\omega\left(\frac{R_0}{R_0} - \frac{R}{R}\right) + \ln \frac{1-e^{-2\pi \frac{R_0}{R_0}\omega}}{1-e^{-2\pi \frac{R}{R}\omega}}}{\bar{\omega}} \right)^{-\frac{8f}{5f+2}} \quad (32)
\end{aligned}$$

and

$$\begin{aligned}
\eta &= \frac{2-f}{fA} \left( \frac{\ln \langle B \rangle - \ln \langle B_0 \rangle}{\bar{\omega}} \right)^{-\frac{8f}{5f+2}} = \\
& \frac{2-f}{fA} \left( \frac{\ln \frac{e^{-2\pi r_{horizon}\omega}}{1-e^{-2\pi r_{horizon}\omega}} - \ln \frac{e^{-2\pi r_{0,horizon}\omega}}{1-e^{-2\pi r_{0,horizon}\omega}}}{\bar{\omega}} \right)^{-\frac{8f}{5f+2}} \sim \\
& \frac{2-f}{fA} \left( \frac{-2\pi\omega(r_{horizon} - r_{0,horizon}) + \ln \frac{1-e^{-2\pi r_{0,horizon}\omega}}{1-e^{-2\pi r_{horizon}\omega}}}{\bar{\omega}} \right) \sim \\
& \frac{2-f}{fA} \left( \frac{2\pi\omega\left(\frac{R_0}{R_0} - \frac{R}{R}\right) + \ln \frac{1-e^{-2\pi \frac{R_0}{R_0}\omega}}{1-e^{-2\pi \frac{R}{R}\omega}}}{\bar{\omega}} \right)^{-\frac{8f}{5f+2}} \quad (33)
\end{aligned}$$

respectively. These parameters depend on the orbital radial distance between the branes. With a decrease in this distance, more inflatons are radiated from the apparent horizon of the system, the slow-roll parameters increase, and as a result, the universe inflates more.

The energy density of radiation in this case has the following form:

$$\begin{aligned}
\rho_\gamma &= 3(1-f)fA \left( \frac{\ln \langle B \rangle - \ln \langle B_0 \rangle}{\bar{\omega}} \right)^{\frac{8f-2}{5f+2}} = \\
& 3(1-f)fA \left( \frac{\ln \frac{e^{-2\pi r_{horizon}\omega}}{1-e^{-2\pi r_{horizon}\omega}} - \ln \frac{e^{-2\pi r_{0,horizon}\omega}}{1-e^{-2\pi r_{0,horizon}\omega}}}{\bar{\omega}} \right)^{\frac{8f-2}{5f+2}} \sim \\
& 3(1-f)fA \left( \frac{-2\pi\omega(r_{horizon} - r_{0,horizon}) + \ln \frac{1-e^{-2\pi r_{0,horizon}\omega}}{1-e^{-2\pi r_{horizon}\omega}}}{\bar{\omega}} \right)^{\frac{8f-2}{5f+2}} \sim \\
& 3(1-f)fA \left( \frac{2\pi\omega\left(\frac{R_0}{R_0} - \frac{R}{R}\right) + \ln \frac{1-e^{-2\pi \frac{R_0}{R_0}\omega}}{1-e^{-2\pi \frac{R}{R}\omega}}}{\bar{\omega}} \right)^{\frac{8f-2}{5f+2}} \quad (34)
\end{aligned}$$

According to this result, the radiation energy density is given in terms of the orbital radius of the brane motion in extra dimensions. As the interaction potential increases, the effect of the inflaton radiation from the apparent horizon in the brane-antibrane system on cosmic inflation becomes systematically more effective because at higher energies there exist more channels for inflaton production.

Using Eqs. (30) and (31), the number of e-folds between the two fields  $B_1$  and  $\mathbf{B}$  is given by:

$$\begin{aligned}
N &= A\left[\left(\frac{\ln \langle B \rangle - \ln \langle B_0 \rangle}{\bar{\omega}}\right)^{-\frac{8f}{5f+2}} - \left(\frac{\ln \langle B_1 \rangle - \ln \langle B_0 \rangle}{\bar{\omega}}\right)^{-\frac{8f}{5f+2}}\right] = \\
&A\left[\left(\frac{\ln \frac{e^{-2\pi r_{horizon}\omega}}{1-e^{-2\pi r_{horizon}\omega}} - \ln \frac{e^{-2\pi r_{0,horizon}\omega}}{1-e^{-2\pi r_{0,horizon}\omega}}}{\bar{\omega}}\right)^{-\frac{8f}{5f+2}} - \right. \\
&\left.\left(\frac{\ln \frac{e^{-2\pi r_{1,horizon}\omega}}{1-e^{-2\pi r_{1,horizon}\omega}} - \ln \frac{e^{-2\pi r_{0,horizon}\omega}}{1-e^{-2\pi r_{0,horizon}\omega}}}{\bar{\omega}}\right)^{-\frac{8f}{5f+2}}\right] \sim \\
&A\left[\left(\frac{-2\pi\omega(r_{horizon} - r_{0,horizon}) + \ln \frac{1-e^{-2\pi r_{0,horizon}\omega}}{1-e^{-2\pi r_{horizon}\omega}}}{\bar{\omega}}\right)^{-\frac{8f}{5f+2}} - \right. \\
&\left.\left(\frac{-2\pi\omega(r_{1,horizon} - r_{0,horizon}) + \ln \frac{1-e^{-2\pi r_{0,horizon}\omega}}{1-e^{-2\pi r_{1,horizon}\omega}}}{\bar{\omega}}\right)^{-\frac{8f}{5f+2}}\right] \sim \\
&A\left[\left(\frac{2\pi\omega\left(\frac{R_0}{R_0} - \frac{R}{R}\right) + \ln \frac{1-e^{-2\pi \frac{R_0}{R_0}\omega}}{1-e^{-2\pi \frac{R}{R}\omega}}}{\bar{\omega}}\right)^{-\frac{8f}{5f+2}} - \right. \\
&\left.\left(\frac{2\pi\omega\left\{\left(\frac{R_0}{R_0} - \frac{R_1}{R_1}\right) + \ln \frac{1-e^{-2\pi \frac{R_0}{R_0}\omega}}{1-e^{-2\pi \frac{R_1}{R_1}\omega}}\right\}}{\bar{\omega}}\right)^{-\frac{8f}{5f+2}}\right] \quad (35)
\end{aligned}$$

This equation depends on the  $\langle B_1 \rangle$  and  $\langle B_0 \rangle$ . To obtain the explicit form of the number of e-folds in terms of the orbital radius distance between the branes, we should find the relation between  $\langle B_1 \rangle$  and  $\langle B_0 \rangle$ . At the beginning of the inflation period where  $\epsilon = 1$ , the inflaton in terms of constant parameters of the model is:

$$\begin{aligned}
\langle B_1 \rangle &= \langle B_0 \rangle \exp\left(\bar{\omega}\left(\frac{1-f}{fA}\right)^{\frac{5f+2}{8f}}\right) \rightarrow \\
\frac{e^{-2\pi r_{1,horizon}\omega}}{1-e^{-2\pi r_{1,horizon}\omega}} &= \frac{e^{-2\pi r_{0,horizon}\omega}}{1-e^{-2\pi r_{0,horizon}\omega}} \exp\left(\bar{\omega}\left(\frac{1-f}{fA}\right)^{\frac{5f+2}{8f}}\right) \rightarrow \\
(r_{1,horizon})^{-1} &\sim (r_{0,horizon})^{-1} \exp\left(\bar{\omega}\left(\frac{1-f}{fA}\right)^{\frac{5f+2}{8f}}\right) - 1 \quad (36)
\end{aligned}$$

From the above equations, we obtain the inflaton ( $\mathbf{B}(t)$ ) and the distance between the two branes ( $R(t)$ ) in terms of number of e-folds

$$\begin{aligned}
\langle B(t) \rangle &= \langle B_0 \rangle \exp\left(\bar{\omega}\left(\frac{N}{A} + \frac{1-f}{fA}\right)^{\frac{5f+2}{8f}}\right) \rightarrow \\
\frac{e^{-2\pi r_{horizon}\omega}}{1-e^{-2\pi r_{horizon}\omega}} &= \frac{e^{-2\pi r_{0,horizon}\omega}}{1-e^{-2\pi r_{0,horizon}\omega}} \exp\left(\bar{\omega}\left(\frac{N}{A} + \frac{1-f}{fA}\right)^{\frac{5f+2}{8f}}\right) \rightarrow \\
(r_{horizon})^{-1} &\sim (r_{0,horizon})^{-1} \exp\left(\bar{\omega}\left(\frac{N}{A} + \frac{1-f}{fA}\right)^{\frac{5f+2}{8f}}\right) - 1 \rightarrow \\
R(t) &= R_0 \exp\left(-\int dt r_{horizon}(N, t)\right) \quad (37)
\end{aligned}$$

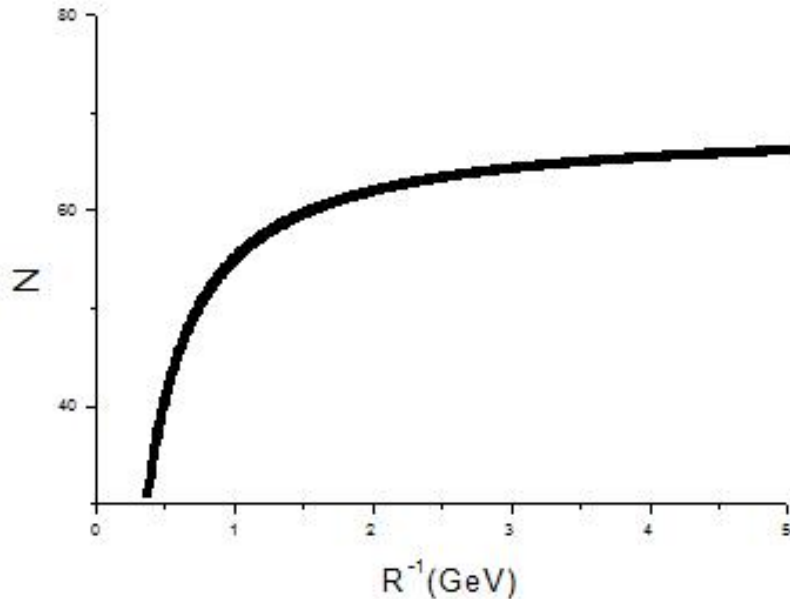


FIG. 1: The number of e-folds  $N$  for intermediate scenario as a function of the  $R^{-1}$  for  $R_0 = 0.45(\text{GeV})^{-1}$ ,  $\omega = 4.6(\text{GeV})$ ,  $\dot{R}_0 = 0.01$ ,  $\dot{R} = 0.1$ ,  $A=1$  and  $f = \frac{1}{2}$ .

This equation shows that the orbital radial distance between the brane universes depends on the number of e-folds. This means that as the distance between the brane decreases, more inflatons are created near the apparent horizon of the brane-antibrane system, and the number of e-folds increases.

In Fig.1 we present the number of e-folds  $N$  for the intermediate scenario as a function of  $R^{-1}$ , where  $R$  is the orbital radial distance between branes. In this plot, we choose  $R_0 = 0.45(\text{GeV})^{-1}$ ,  $\omega = 4.6(\text{GeV})$ ,  $\dot{R}_0 = 0.01$ ,  $\dot{R} = 0.1$ ,  $A=1$  and  $f = \frac{1}{2}$ . It is clear that the number of e-folds  $N$  is much larger for a smaller orbital radial distance between the branes. This is because, as the distance between the branes becomes smaller, the temperature becomes larger and the thermal radiation of the inflatons enhances.

Now, we will consider tensor and scalar perturbations that appear during the inflationary period for the warm inflation model. These perturbations may leave an imprint in the CMB anisotropy and on the LSS [18, 19]. The power spectrum and a spectral index are characteristics of each fluctuation:  $\Delta_R^2(k)$  and  $n_s$  for scalar perturbations,  $\Delta_T^2(k)$  and  $n_T$  for

tensor perturbations. In warm and cool inflation models, the scalar power spectrum is given by [5]:

$$\Delta_R^2 = \left( \frac{H}{\langle \dot{B} \rangle} \langle \delta B \rangle \right)^2 \quad (38)$$

where the thermal fluctuation in the warm inflation model yields [18, 19]:

$$\langle \delta B \rangle = \left( \frac{\Gamma H T^2}{(4\pi)^3} \right)^{\frac{1}{4}} \quad (39)$$

Using Eqs. (20), (37), (38) and (39), we calculate the scalar power spectrum as:

$$\begin{aligned} \Delta_R^2 &= - \left( \frac{\Gamma_0^3}{36(4\pi)^3} \right)^{\frac{1}{2}} \frac{H^{\frac{3}{2}}}{\dot{H}} = \\ & \left( \frac{\Gamma_0^3}{36(4\pi)^3} \right)^{\frac{1}{2}} \left( \frac{3^{11}(fA)^{15}(1-f)^3}{(2C)^{11}} \right)^{\frac{1}{8}} \langle B \rangle^3 \left( \frac{\ln \langle B \rangle - \ln \langle B_0 \rangle}{\bar{\omega}} \right)^{-\frac{15f-18}{5f+2}} = \\ & \left( \frac{\Gamma_0^3}{36(4\pi)^3} \right)^{\frac{1}{2}} \left( \frac{3^{11}(fA)^{15}(1-f)^3}{(2C)^{11}} \right)^{\frac{1}{8}} \left( \frac{e^{-2\pi r_{horizon}\omega}}{1 - e^{-2\pi r_{horizon}\omega}} \right)^3 \times \\ & \left( \frac{\ln \frac{e^{-2\pi r_{horizon}\omega}}{1 - e^{-2\pi r_{horizon}\omega}} - \ln \frac{e^{-2\pi r_{0,horizon}\omega}}{1 - e^{-2\pi r_{0,horizon}\omega}}}{\bar{\omega}} \right)^{-\frac{15f-18}{5f+2}} \sim \\ & \left( \frac{\Gamma_0^3}{36(4\pi)^3} \right)^{\frac{1}{2}} \left( \frac{3^{11}(fA)^{15}(1-f)^3}{(2C)^{11}} \right)^{\frac{1}{8}} \left( \frac{e^{-2\pi r_{horizon}\omega}}{1 - e^{-2\pi r_{horizon}\omega}} \right)^3 \times \\ & \left( \frac{-2\pi\omega(r_{horizon} - r_{0,horizon}) + \ln \frac{1 - e^{-2\pi r_{0,horizon}\omega}}{1 - e^{-2\pi r_{horizon}\omega}}}{\bar{\omega}} \right)^{-\frac{15f-18}{5f+2}} \sim \\ & \left( \frac{\Gamma_0^3}{36(4\pi)^3} \right)^{\frac{1}{2}} \left( \frac{3^{11}(fA)^{15}(1-f)^3}{(2C)^{11}} \right)^{\frac{1}{8}} \left( \frac{e^{-2\pi \frac{R_0}{R}\omega}}{1 - e^{-2\pi \frac{R_0}{R}\omega}} \right)^3 \times \\ & \left( \frac{2\pi\omega \left( \frac{R_0}{R_0} - \frac{R}{R} \right) + \ln \frac{1 - e^{-2\pi \frac{R_0}{R_0}\omega}}{1 - e^{-2\pi \frac{R_0}{R}\omega}}}{\bar{\omega}} \right)^{-\frac{15f-18}{5f+2}} \quad (40) \end{aligned}$$

where  $k$  is the co-moving wavenumber. With the wavenumber  $k = k_0 = 0.002 Mpc^{-1}$ , the combined measurement from WMAP+BAO+SN of  $\Delta_R^2$  is reported by the WMAP7 data [20] as:

$$\Delta_R^2 = (2.455 \pm 0.096) \times 10^{-19} \quad (41)$$

Using this equation and equation(40), and choosing ( $A=1, f=1/2, \dot{R} = 0.1, \omega = 4.6(GeV), \Gamma_0=1$ ), we obtain the radial distance between our brane and another brane,  $R = (1.5 GeV)^{-1}$ . This result is consistent with previous calculations [21].

Another important perturbation parameter is the spectral index  $n_s$  which is given by:

$$n_s - 1 = - \frac{d \ln \Delta_R^2}{d \ln k} =$$

$$\begin{aligned}
& \frac{15f-18}{8fA} \left( \frac{\ln \langle B \rangle - \ln \langle B_0 \rangle}{\bar{\omega}} \right)^{\frac{-8f}{5f+2}} = \\
& \frac{15f-18}{8fA} \left( \frac{\ln \frac{e^{-2\pi r_{horizon}\omega}}{1-e^{-2\pi r_{horizon}\omega}} - \ln \frac{e^{-2\pi r_{0,horizon}\omega}}{1-e^{-2\pi r_{0,horizon}\omega}}}{\bar{\omega}} \right)^{\frac{-8f}{5f+2}} \sim \\
& \frac{15f-18}{8fA} \left( \frac{-2\pi\omega(r_{horizon} - r_{0,horizon}) + \ln \frac{1-e^{-2\pi r_{0,horizon}\omega}}{1-e^{-2\pi r_{horizon}\omega}}}{\bar{\omega}} \right)^{\frac{-8f}{5f+2}} \sim \\
& \frac{15f-18}{8fA} \left( \frac{2\pi\omega\left(\frac{R_0}{R_0} - \frac{R}{R}\right) + \ln \frac{1-e^{-2\pi\frac{R_0}{R_0}\omega}}{1-e^{-2\pi\frac{R}{R}\omega}}}{\bar{\omega}} \right)^{\frac{-8f}{5f+2}} \quad (42)
\end{aligned}$$

where we have used the thermal distribution in Eq.(20). In Fig. 2 we show the results for the spectral index in the intermediate scenario as a function of  $R^{-1}$ , where  $R$  is the orbital radial distance between the branes. In this plot we choose  $R_0 = 0.45(GeV)^{-1}$ ,  $\omega = 4.6(GeV)$ ,  $\dot{R}_0 = 0.01$ ,  $\dot{R} = 0.1$ ,  $A=1$  and  $f = \frac{1}{2}$ . As can be seen from Fig.2, the spectral index decreases rapidly when the distance between the branes increases. By comparing Fig. 1 and Fig. 2, we find that the  $N \simeq 50$  case leads to  $n_s \simeq 0.96$ . This result is compatible with observational data [5, 20, 22]. At this point, the radial distance between our brane and another brane is  $R = (1.5GeV)^{-1}$ .

Using Eq.(20), we can calculate the tensor power spectrum and its spectral index as:

$$\begin{aligned}
\Delta_T^2 &= \frac{2H^2}{\pi^2} = \\
& \frac{2(fA)^2}{\pi^2} \left( \frac{\ln \langle B \rangle - \ln \langle B_0 \rangle}{\bar{\omega}} \right)^{\frac{16(f-1)}{5f+2}} = \\
& \frac{2(fA)^2}{\pi^2} \left( \frac{\ln \frac{e^{-2\pi r_{horizon}\omega}}{1-e^{-2\pi r_{horizon}\omega}} - \ln \frac{e^{-2\pi r_{0,horizon}\omega}}{1-e^{-2\pi r_{0,horizon}\omega}}}{\bar{\omega}} \right)^{\frac{16(f-1)}{5f+2}} \sim \\
& \frac{2(fA)^2}{\pi^2} \left( \frac{-2\pi\omega(r_{horizon} - r_{0,horizon}) + \ln \frac{1-e^{-2\pi r_{0,horizon}\omega}}{1-e^{-2\pi r_{horizon}\omega}}}{\bar{\omega}} \right)^{\frac{16(f-1)}{5f+2}} \sim \\
& \frac{2(fA)^2}{\pi^2} \left( \frac{2\pi\omega\left(\frac{R_0}{R_0} - \frac{R}{R}\right) + \ln \frac{1-e^{-2\pi\frac{R_0}{R_0}\omega}}{1-e^{-2\pi\frac{R}{R}\omega}}}{\bar{\omega}} \right)^{\frac{16(f-1)}{5f+2}} \quad (43)
\end{aligned}$$

$$\begin{aligned}
n_T &= -2\varepsilon = \\
& -\frac{2-2f}{fA} \left( \frac{\ln \langle B \rangle - \ln \langle B_0 \rangle}{\bar{\omega}} \right)^{\frac{-8f}{5f+2}} = \\
& -\frac{2-2f}{fA} \left( \frac{\ln \frac{e^{-2\pi r_{horizon}\omega}}{1-e^{-2\pi r_{horizon}\omega}} - \ln \frac{e^{-2\pi r_{0,horizon}\omega}}{1-e^{-2\pi r_{0,horizon}\omega}}}{\bar{\omega}} \right)^{\frac{-8f}{5f+2}} \sim \\
& -\frac{2-2f}{fA} \left( \frac{-2\pi\omega(r_{horizon} - r_{0,horizon}) + \ln \frac{1-e^{-2\pi r_{0,horizon}\omega}}{1-e^{-2\pi r_{horizon}\omega}}}{\bar{\omega}} \right)^{\frac{-8f}{5f+2}} \sim
\end{aligned}$$

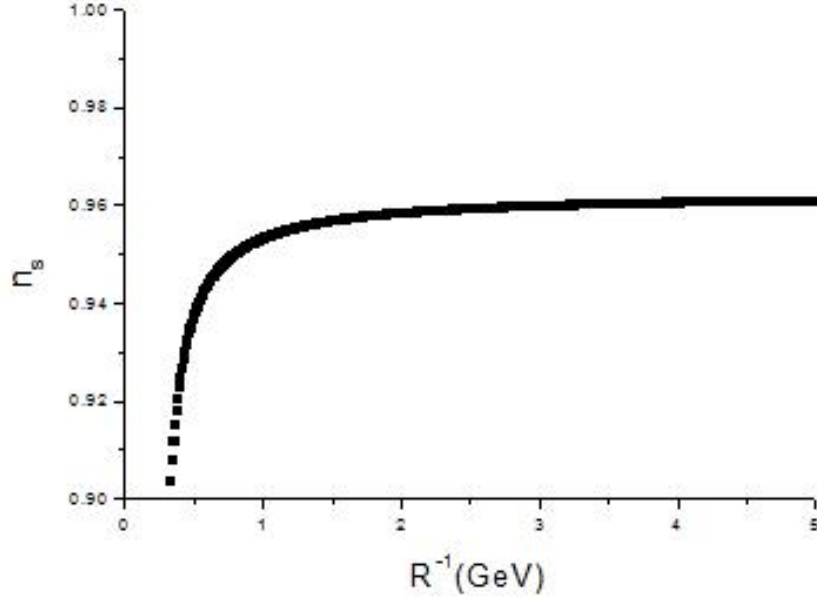


FIG. 2: The spectral index in intermediate scenario as a function of  $R^{-1}$  for  $R_0 = 0.45(\text{GeV})^{-1}$ ,  $\omega = 4.6(\text{GeV})$ ,  $\dot{R}_0 = 0.01$ ,  $\dot{R} = 0.1$ ,  $A=1$  and  $f = \frac{1}{2}$ .

$$-\frac{2-2f}{fA} \left( \frac{2\pi\omega \left( \frac{R_0}{R_0} - \frac{R}{R} \right) + \ln \frac{1-e^{-2\pi \frac{R_0}{R_0} \omega}}{1-e^{-2\pi \frac{R}{R} \omega}}}{\bar{\omega}} \right)^{\frac{-8f}{5f+2}} \quad (44)$$

These perturbations depend on the orbital radial distance between the branes. As we discussed before, these perturbations have a direct effect on the cosmic microwave background (CMB). Thus, we can observe the signature of interaction between the branes by means of observational data.

Another important parameter is the tensor-scalar ratio that has the following form:

$$\begin{aligned} R_{\text{Tensor-scalar}} &= - \left( \frac{144(4\pi)^3 (fA)^4}{\Gamma_0^3 \pi^4 T^2} \right)^{\frac{1}{2}} \dot{H} H^{\frac{1}{2}} = \\ & \left( \frac{144(4\pi)^3 (fA)^4}{\Gamma_0^3 \pi^4} \right)^{\frac{1}{2}} \left( \frac{3^{11} (fA)^{15} (1-f)^3}{(2C)^{11}} \right)^{\frac{1}{8}} \times \\ & \langle B \rangle^3 \left( \frac{\ln \langle B \rangle - \ln \langle B_0 \rangle}{\bar{\omega}} \right)^{\frac{f+2}{5f+2}} = \\ & \left( \frac{144(4\pi)^3 (fA)^4}{\Gamma_0^3 \pi^4} \right)^{\frac{1}{2}} \left( \frac{3^{11} (fA)^{15} (1-f)^3}{(2C)^{11}} \right)^{\frac{1}{8}} \left( \frac{e^{-2\pi r_{\text{horizon}} \omega}}{1 - e^{-2\pi r_{\text{horizon}} \omega}} \right)^3 \times \end{aligned}$$

$$\begin{aligned}
& \left( \frac{\ln \frac{e^{-2\pi r_{horizon}\omega}}{1-e^{-2\pi r_{horizon}\omega}} - \ln \frac{e^{-2\pi r_{0,horizon}\omega}}{1-e^{-2\pi r_{0,horizon}\omega}}}{\bar{\omega}} \right)^{\frac{f+2}{5f+2}} \sim \\
& \left( \frac{144(4\pi)^3(fA)^4}{\Gamma_0^3\pi^4} \right)^{\frac{1}{2}} \left( \frac{3^{11}(fA)^{15}(1-f)^3}{(2C)^{11}} \right)^{\frac{1}{8}} \left( \frac{e^{-2\pi r_{horizon}\omega}}{1-e^{-2\pi r_{horizon}\omega}} \right)^3 \times \\
& \left( \frac{-2\pi\omega(r_{horizon} - r_{0,horizon}) + \ln \frac{1-e^{-2\pi r_{0,horizon}\omega}}{1-e^{-2\pi r_{horizon}\omega}}}{\bar{\omega}} \right)^{\frac{f+2}{5f+2}} \sim \\
& \left( \frac{144(4\pi)^3(fA)^4}{\Gamma_0^3\pi^4} \right)^{\frac{1}{2}} \left( \frac{3^{11}(fA)^{15}(1-f)^3}{(2C)^{11}} \right)^{\frac{1}{8}} \left( \frac{e^{-2\pi \frac{R}{R_0}\omega}}{1-e^{-2\pi \frac{R}{R_0}\omega}} \right)^3 \times \\
& \left( \frac{2\pi\omega\left(\frac{R_0}{R_0} - \frac{R}{R}\right) + \ln \frac{1-e^{-2\pi \frac{R_0}{R_0}\omega}}{1-e^{-2\pi \frac{R}{R_0}\omega}}}{\bar{\omega}} \right)^{\frac{f+2}{5f+2}} \tag{45}
\end{aligned}$$

In Fig. 3 we present the tensor-scalar ratio in the intermediate scenario as a function of  $R^{-1}$ , where  $R$  is the orbital radial distance between the branes. In this plot we choose  $R_0 = 0.45(GeV)^{-1}$ ,  $\omega = 4.6(GeV)$ ,  $\dot{R}_0 = 0.01$ ,  $\dot{R} = 0.1$ ,  $C=70$ ,  $\Gamma_0 = 1$ ,  $A=1$  and  $f = \frac{1}{2}$ . We observe that as the orbital radius distance between branes increases, the tensor-scalar ratio increases. By comparing Figs. 2 and 3, we notice that the standard case  $n_s \simeq 0.96$ , may be found in  $0.01 < R_{Tensor-scalar} < 0.22$ , which agrees with observational data [5, 20, 22]. At this stage, the radial distance between our brane and another brane is  $R = (1.5GeV)^{-1}$ .

Now, we would like to consider the signature of interaction between branes in the context of logamediate inflation with scale factor:

$$a(t) = a_0 \exp(A[\ln t]^\lambda) \tag{46}$$

where  $A$  is a constant parameter. This model is converted to power-law inflation for the  $\lambda = 1$  case. This scenario is applied for a number of scalar-tensor theories [13]. The effective potential of this solution is used in dark energy models [23], supergravity, Kaluza-Klein theories and super-string models [13, 24]. The number of e-folds in this case is given by [5]:

$$N = \int_{t_1}^t H dt = A([\ln t]^\lambda - [\ln t_1]^\lambda) \tag{47}$$

where  $t_1$  is the begining time of inflation. From Eqs. (20), (24), (25), (26), (27) and (46) we may find the inflaton  $\mathbf{B}$  and also the orbital radial distance between the two branes:

$$\begin{aligned}
& \ln \langle B \rangle - \ln \langle B_0 \rangle = \tilde{\omega} \Xi(t) \rightarrow \\
& \ln \frac{e^{-2\pi r_{horizon}\omega}}{1-e^{-2\pi r_{horizon}\omega}} - \ln \frac{e^{-2\pi r_{0,horizon}\omega}}{1-e^{-2\pi r_{0,horizon}\omega}} = \tilde{\omega} \Xi(t) \rightarrow
\end{aligned}$$



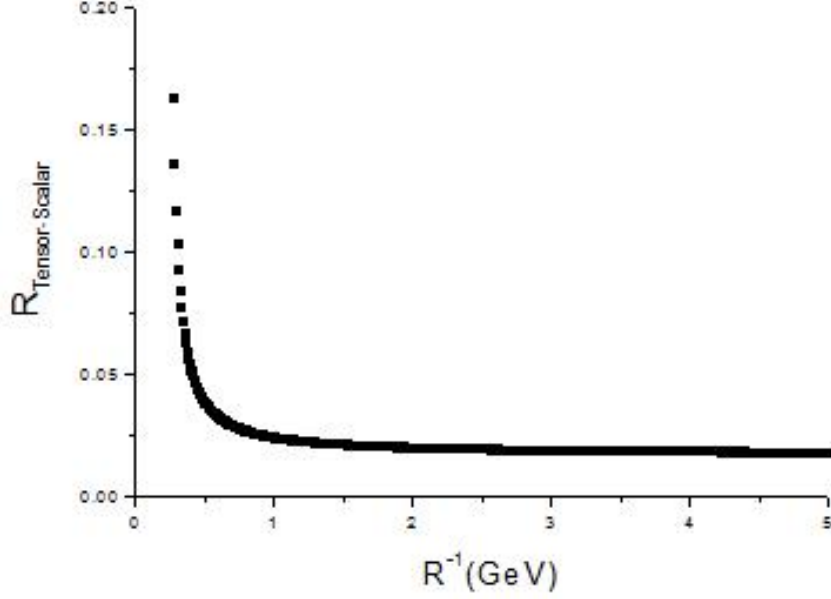


FIG. 3: The tensor-scalar ratio in intermediate scenario as a function of  $R^{-1}$  for  $R_0 = 0.45(\text{GeV})^{-1}$ ,  $\omega = 4.6(\text{GeV})$ ,  $\dot{R}_0 = 0.01$ ,  $\dot{R} = 0.1$ ,  $A=1$  and  $f = \frac{1}{2}$ .

$$\begin{aligned}
 & -2\pi\omega(r_{\text{horizon}} - r_{0,\text{horizon}}) + \ln \frac{1 - e^{-2\pi r_{0,\text{horizon}}\omega}}{1 - e^{-2\pi r_{\text{horizon}}\omega}} \sim \tilde{\omega}\Xi(t) \rightarrow \\
 & (2\pi\omega(\frac{R_0}{\dot{R}_0} - \frac{R}{\dot{R}}) + \ln \frac{1 - e^{-2\pi \frac{R_0}{R_0}\omega}}{1 - e^{-2\pi \frac{R}{R}\omega}}) \sim \tilde{\omega}\Xi(t)
 \end{aligned} \tag{48}$$

where  $\tilde{\omega} = (\frac{6}{\Gamma_0}(\frac{2C}{3})^{\frac{3}{4}})^{\frac{1}{2}}((-4)^{5\lambda+3}(\lambda A)^5)^{\frac{1}{8}}$  and  $\Xi(t) = \gamma[\frac{5\lambda+3}{8}, \frac{\ln t}{4}]$  ( $\gamma$  is the incomplete gamma function [25]). The potential in terms of the orbital radial distance between the two branes is presented as:

$$\begin{aligned}
 V &= \frac{2\lambda^2 A^2 [\ln(\Xi^{-1}(\frac{\ln\langle B \rangle - \ln\langle B_0 \rangle}{\tilde{\omega}}))]^{2\lambda-2}}{(\Xi^{-1}(\frac{\ln\langle B \rangle - \ln\langle B_0 \rangle}{\tilde{\omega}}))^2} = \\
 & \frac{2\lambda^2 A^2 [\ln(\Xi^{-1}(\frac{(2\pi\omega(\frac{R_0}{\dot{R}_0} - \frac{R}{\dot{R}}) + \ln \frac{1 - e^{-2\pi \frac{R_0}{R_0}\omega}}{1 - e^{-2\pi \frac{R}{R}\omega}})}{\tilde{\omega}}))]^{2\lambda-2}}{(\Xi^{-1}(\frac{(2\pi\omega(\frac{R_0}{\dot{R}_0} - \frac{R}{\dot{R}}) + \ln \frac{1 - e^{-2\pi \frac{R_0}{R_0}\omega}}{1 - e^{-2\pi \frac{R}{R}\omega}})}{\tilde{\omega}}))^2}
 \end{aligned} \tag{49}$$

This equation shows that the inflatonic potential on our brane depends on the orbital radial distance and the interaction potential between the two branes. In fact, the interaction

between branes causes inflation of our universe.

Now, we obtain the slow-roll parameters of the model in this case:

$$\begin{aligned}\epsilon &= \frac{[\ln(\Xi^{-1}(\frac{(2\pi\omega(\frac{R_0}{R_0}-\frac{R}{R})+\ln\frac{1-e^{-2\pi\frac{R_0}{R_0}\omega}}{1-e^{-2\pi\frac{R}{R}\omega}})}{\tilde{\omega}})))]^{1-\lambda}}{\lambda A} \\ \eta &= \frac{2[\ln(\Xi^{-1}(\frac{(2\pi\omega(\frac{R_0}{R_0}-\frac{R}{R})+\ln\frac{1-e^{-2\pi\frac{R_0}{R_0}\omega}}{1-e^{-2\pi\frac{R}{R}\omega}})}{\tilde{\omega}})))]^{1-\lambda}}{\lambda A}\end{aligned}\quad (50)$$

In this case, like the intermediate case, as the distance between the branes decreases, more inflatons are created in the brane-antibrane system, the slow-roll parameters increase, and the universe inflates.

Using Eqs (20), (47) and (48), the number of e-folds between the two fields  $B_1$  and  $\mathbf{B}(t)$  can be obtained as:

$$\begin{aligned}N &= A([\ln(\Xi^{-1}(\frac{(2\pi\omega(\frac{R_0}{R_0}-\frac{R}{R})+\ln\frac{1-e^{-2\pi\frac{R_0}{R_0}\omega}}{1-e^{-2\pi\frac{R}{R}\omega}})}{\tilde{\omega}})))]^\lambda \\ &\quad - [\ln(\Xi^{-1}(\frac{(2\pi\omega(\frac{R_0}{R_0}-\frac{R_1}{R_1})+\ln\frac{1-e^{-2\pi\frac{R_0}{R_0}\omega}}{1-e^{-2\pi\frac{R_1}{R_1}\omega}})}{\tilde{\omega}})))]^\lambda = \\ &= A([\ln(\Xi^{-1}(\frac{(2\pi\omega(\frac{R_0}{R_0}-\frac{R}{R})+\ln\frac{1-e^{-2\pi\frac{R_0}{R_0}\omega}}{1-e^{-2\pi\frac{R}{R}\omega}})}{\tilde{\omega}})))]^\lambda - [\lambda A]^\frac{\lambda}{1-\lambda}\end{aligned}\quad (51)$$

where  $R_1$  is the the orbital radial distance between the two branes at the beginning of the inflationary epoch when ( $\epsilon = 1$ ). Using the above equation, the orbital radial distance between the two branes in the inflationary period could be obtained in terms of the number of e-folds as:

$$R - R_0 = \frac{\tilde{\omega} \dot{R}^2 \dot{R}_0^2}{2\pi\omega} \Xi [\exp(\frac{N}{A} + (\lambda A)^\frac{\lambda}{1-\lambda})^\frac{1}{\lambda}] \quad (52)$$

This equation shows that, in this case, like the intermediate case, the number of e-fields depends on the orbital radial distance between the branes. This is because as the distance between the branes decreases, the number of inflatons, which has direct effects on the number of e-folds, increases.

Also, the scalar and tensor power spectrum in this case are given by:

$$\Delta_R^2 = (\frac{\Gamma_0^3}{36(4\pi)^3})^\frac{1}{2} (\frac{3^{11}(\lambda A)^{15}}{(2C)^{11}})^\frac{1}{8} (\frac{e^{-2\pi r_{horizon}\omega}}{1 - e^{-2\pi r_{horizon}\omega}})^{-3}$$

$$\begin{aligned}
& \times \exp\left(-\frac{15}{8} \left[ \ln\left(\Xi^{-1}\left(\frac{(2\pi\omega(\frac{R_0}{R_0} - \frac{R}{R}) + \ln \frac{1-e^{-2\pi\frac{R_0}{R_0}\omega}}{1-e^{-2\pi\frac{R}{R}\omega}})}{\tilde{\omega}}\right)\right)\right]\right) \\
& \times \left[ \left[ \ln\left(\Xi^{-1}\left(\frac{(2\pi\omega(\frac{R_0}{R_0} - \frac{R}{R}) + \ln \frac{1-e^{-2\pi\frac{R_0}{R_0}\omega}}{1-e^{-2\pi\frac{R}{R}\omega}})}{\tilde{\omega}}\right)\right)\right]^\lambda \right]^{15\frac{\lambda-1}{8\lambda}} \\
& \times \exp\left(-3\tilde{\omega}\Xi\left(\exp\left(\ln\left(\Xi^{-1}\left(\frac{(2\pi\omega(\frac{R_0}{R_0} - \frac{R}{R}) + \ln \frac{1-e^{-2\pi\frac{R_0}{R_0}\omega}}{1-e^{-2\pi\frac{R}{R}\omega}})}{\tilde{\omega}}\right)\right)\right)\right)\right) \tag{53}
\end{aligned}$$

$$\begin{aligned}
\Delta_T^2 = & \frac{2\lambda^2 A^2 \left[ \ln\left(\Xi^{-1}\left(\frac{(2\pi\omega(\frac{R_0}{R_0} - \frac{R}{R}) + \ln \frac{1-e^{-2\pi\frac{R_0}{R_0}\omega}}{1-e^{-2\pi\frac{R}{R}\omega}})}{\tilde{\omega}}\right)\right)\right]^{2-2\lambda}}{\pi^2 \left(\Xi^{-1}\left(\frac{(2\pi\omega(\frac{R_0}{R_0} - \frac{R}{R}) + \ln \frac{1-e^{-2\pi\frac{R_0}{R_0}\omega}}{1-e^{-2\pi\frac{R}{R}\omega}})}{\tilde{\omega}}\right)\right)^2} \tag{54}
\end{aligned}$$

These spectra in the context of logamediate inflation, like intermediate inflation, change with an increase or decrease in the orbital radial distance between the branes. The spectral index in this case has the following forms:

$$\begin{aligned}
n_s - 1 = & -\frac{15(\lambda - 1)}{8\lambda A} \left[ \left[ \ln\left(\Xi^{-1}\left(\frac{(2\pi\omega(\frac{R_0}{R_0} - \frac{R}{R}) + \ln \frac{1-e^{-2\pi\frac{R_0}{R_0}\omega}}{1-e^{-2\pi\frac{R}{R}\omega}})}{\tilde{\omega}}\right)\right)\right]^\lambda \right]^{-1} \\
n_T = & -\frac{2 \left[ \ln\left(\Xi^{-1}\left(\frac{(2\pi\omega(\frac{R_0}{R_0} - \frac{R}{R}) + \ln \frac{1-e^{-2\pi\frac{R_0}{R_0}\omega}}{1-e^{-2\pi\frac{R}{R}\omega}})}{\tilde{\omega}}\right)\right)\right]^{1-\lambda}}{\lambda A} \tag{55}
\end{aligned}$$

In Figs. 4 and 5, we present the number of e-folds  $N$  and the spectral index for the logamediate inflation scenario as a function of  $R^{-1}$ , where  $R$  is the orbital radial distance between the branes. In these plots, we choose  $R_0 = 0.45(GeV)^{-1}$ ,  $\omega = 4.6(GeV)$ ,  $\dot{R}_0 = 0.01$ ,  $\dot{R} = 0.1$ ,  $\lambda = 10$ ,  $A=1$  and  $f = \frac{1}{2}$ . In this case, like the intermediate case, we find that the number of e-folds  $N$  and the spectral index are much larger for smaller orbital radial distance between branes. This is because, as the distance between the branes becomes smaller, the temperature becomes larger, and the thermal radiation of the inflatons enhances.

Finally, we could find the tensor-scalar ratio in terms of the orbital radial distance between two branes:

$$\begin{aligned}
R_{Tensor-scalar} = & \left(\frac{144(4\pi)^3}{\Gamma_0^3 \pi^4}\right)^{\frac{1}{2}} \left(\frac{(2C)^{11}(\lambda A)}{3^{11}}\right)^{\frac{1}{8}} \left(\frac{e^{-2\pi r_{0,horizon}\omega}}{1 - e^{-2\pi r_{0,horizon}\omega}}\right)^3 \\
& \times \exp\left(-\frac{1}{8} \left[ \ln\left(\Xi^{-1}\left(\frac{(2\pi\omega(\frac{R_0}{R_0} - \frac{R}{R}) + \ln \frac{1-e^{-2\pi\frac{R_0}{R_0}\omega}}{1-e^{-2\pi\frac{R}{R}\omega}})}{\tilde{\omega}}\right)\right)\right]\right)
\end{aligned}$$

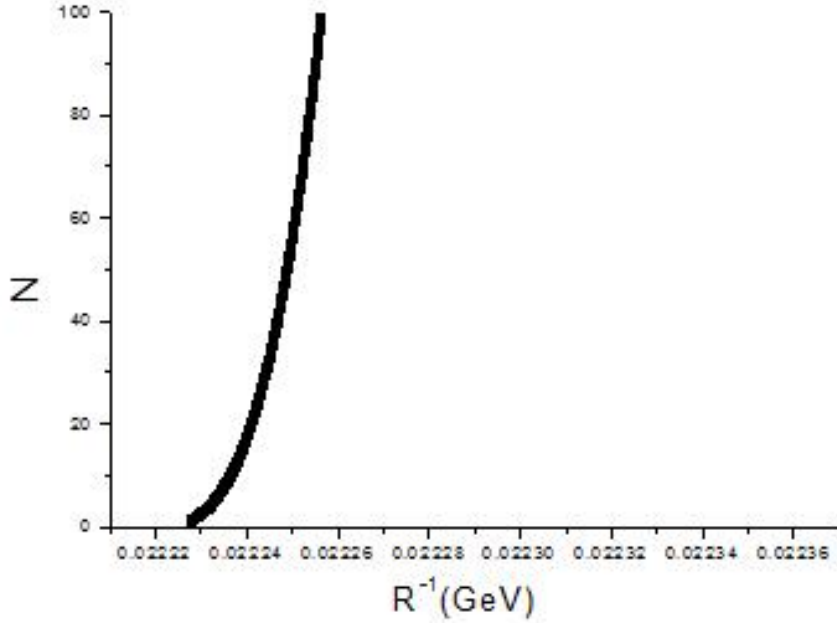


FIG. 4: The number of e-folds  $N$  in logamediate inflation scenario as a function of  $R^{-1}$  for  $R_0 = 0.45(\text{GeV})^{-1}$ ,  $\omega = 4.6(\text{GeV})$ ,  $\dot{R}_0 = 0.01$ ,  $\dot{R} = 0.1$ ,  $\lambda = 10$ ,  $A=1$  and  $f = \frac{1}{2}$ .

$$\begin{aligned}
& \times \left[ \left[ \ln \left( \Xi^{-1} \left( \frac{2\pi\omega \left( \frac{R_0}{R_0} - \frac{R}{R} \right) + \ln \frac{1-e^{-2\pi \frac{R_0}{R_0} \omega}}{1-e^{-2\pi \frac{R}{R} \omega}}}{\tilde{\omega}} \right) \right) \right]^\lambda \right]^{\frac{-31(\lambda-1)}{8\lambda}} \\
& \times \exp(3\tilde{\omega}\Xi[\exp(\ln(\Xi^{-1}(\frac{2\pi\omega(\frac{R_0}{R_0} - \frac{R}{R}) + \ln \frac{1-e^{-2\pi \frac{R_0}{R_0} \omega}}{1-e^{-2\pi \frac{R}{R} \omega}}}{\tilde{\omega}})))))) \quad (56)
\end{aligned}$$

In Fig. 6 we present the tensor-scalar ratio in the logamediate scenario as a function of  $R^{-1}$ , where  $R$  is the orbital radial distance between the branes. In this plot we choose  $R_0 = 0.45(\text{GeV})^{-1}$ ,  $\omega = 4.6(\text{GeV})$ ,  $\dot{R}_0 = 0.01$ ,  $\dot{R} = 0.1$ ,  $C=70$ ,  $\Gamma_0 = 1$ ,  $\lambda = 10$ ,  $A=1$  and  $f = \frac{1}{2}$ . In this case, like the intermediate case, with an increase in the orbital radial distance between branes, the tensor-scalar ratio increases. By comparing Figs. 5 and 6, we notice that the standard case  $n_s \simeq 0.96$ , may be found in  $0.01 < R_{\text{tensor-scalar}} < 0.22$ , which agrees with observational data [5, 20, 22]. At this stage, the radial distance between our brane and another brane is  $R = (0.02225\text{GeV})^{-1}$ .

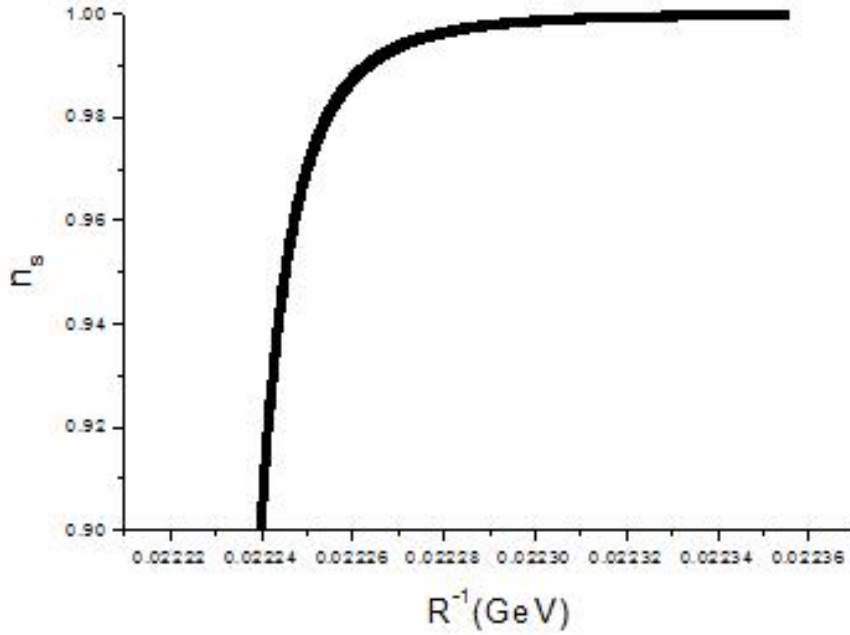


FIG. 5: The spectral index in logamediate inflation scenario as a function of  $R^{-1}$  for  $R_0 = 0.45(\text{GeV})^{-1}$ ,  $\omega = 4.6(\text{GeV})$ ,  $\dot{R}_0 = 0.01$ ,  $\dot{R} = 0.1$ ,  $\lambda = 10$ ,  $A=1$  and  $f = \frac{1}{2}$ .

#### IV. SUMMARY AND DISCUSSION

In this research, we calculate the thermal distribution of inflatons near the apparent horizon in a brane-antibrane system, and show that the energy density, slow-roll, number of e-folds and perturbation parameters can be given in terms of the orbital radius of the brane motion in extra dimensions. According to our results, when the distance between branes increases, the number of e-folds and the spectral index for both intermediate and logamediate models decrease rapidly; however the tensor-scalar ratio increases. This is because, as the separate distance between branes decreases, the interaction potential increases, and at higher energies, there exist more channels for inflaton production near the apparent horizon in the brane-antibrane system; consequently, the effect of inflaton radiation from this horizon on cosmic inflation becomes systematically more effective. We find that the  $N \simeq 50$  case leads to  $n_s \simeq 0.96$ . This standard case may be found in  $0.01 < R_{\text{tensor-scalar}} < 0.22$ , which agrees with observational data [5, 20, 22] (We note some new observational data has been obtained, but we believe that our models will fit this as well. This work is under progress). At this

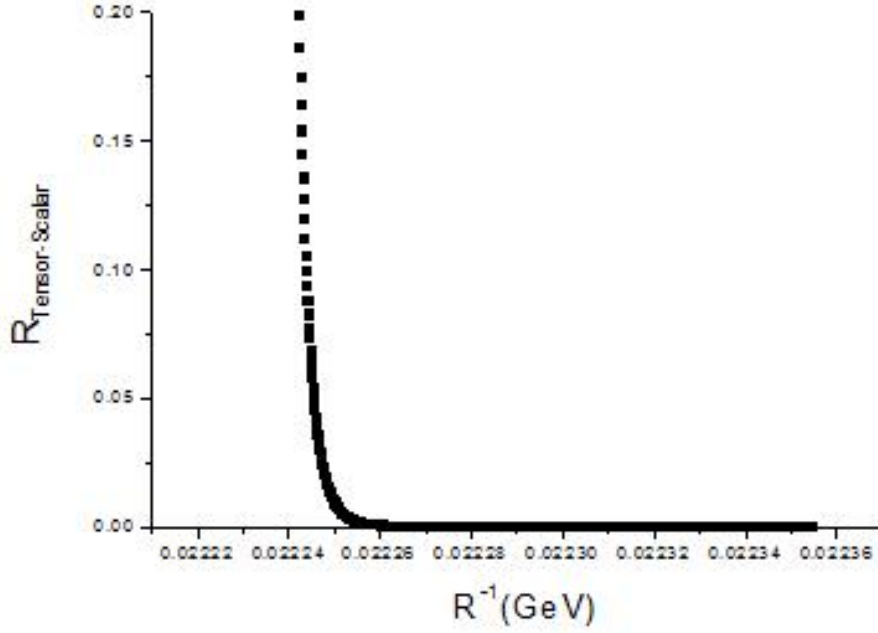


FIG. 6: The tensor-scalar ratio in logamediate inflation scenario as a function of  $R^{-1}$  for  $R_0 = 0.45(GeV)^{-1}$ ,  $\omega = 4.6(GeV)$ ,  $\dot{R}_0 = 0.01$ ,  $\dot{R} = 0.1$ ,  $\lambda = 10$ ,  $A=1$  and  $f = \frac{1}{2}$ .

point, the radial distance between our brane and another brane is  $R = (1.5GeV)^{-1}$  in the intermediate model and  $R = (0.02225GeV)^{-1}$  in the logamediate model.

There is no underlying data that is necessary for this work, and there is no special funding.

The author declares that there is no conflict of interest regarding the publication of this paper

- 
- [1] Salvador Robles-Perez, Pedro F. Gonzalez-Diaz, Phys. Rev. D81: 083529, (2010).
  - [2] Pedro F. Gonzalez-Diaz, Salvador Robles-Perez, Phys. Lett. B679: 298-301, (2009).
  - [3] Alireza Sepeshri, Somayyeh Shoorvazi, Mohammad Ebrahim Zomorrodian, Can. J. Phys., 91: 256-259, (2013)/ Can. J. Phys. 87, 1151-1158 (2009).
  - [4] Yin-Zhe Ma, Qing-Guo Huang, Xin Zhang, , Phys. Rev. D., 87, 103516, (2013).
  - [5] Mar Bastero-Gil, Arjun Berera, Int. J. Mod. Phys. A 24: 2207-2240, (2009).
  - [6] N. D. Birrell and P. C. W. Davies, Quantum fields in curved space (Cambridge University

- Press, New York, 1982).
- [7] Doyeol Ahn, Phys. Rev. D74: 084010, (2006).
  - [8] A. Sepehri, S. Shoovazi, Astrophysics and Space Science, 344, 521-527, (2013).
  - [9] M. Bastero-Gil, A. Berera and R. O. Ramos, JCAP 1109, 033 (2011).
  - [10] M. Bastero-Gil, A. Berera, R. O. Ramos and J. G. Rosa, JCAP 1301, 016 (2013).
  - [11] A. Berera, Phys. Rev. Lett. 75, 3218 (1995) [astro-ph/9509049]; Phys. Rev. D55, 3346 (1997) [hep-ph/9612239].
  - [12] J. D. Barrow, Class. Quantum Grav. 13, 2965 (1996).
  - [13] J. D. Barrow, Phys. Rev. D 51, 2729 (1995).
  - [14] Mar Bastero-Gil Arjun Berera, Phys. Rev. D76: 043515, 2007.
  - [15] J. Yokoyama and K. Maeda, Phys. Lett. B207, 31, (1988).
  - [16] J. D. Barrow, Phys. Lett. B235, 40 (1990); J. D. Barrow and P. Saich, Phys. Lett. B249, 406 (1990).
  - [17] J. D. Barrow, A. R. Liddle, Phys. Rev. D47, 5219, (1993).
  - [18] A. H. Guth and S. Y. Pi, Phys. Rev. Lett. 49, 1110 (1982).
  - [19] V. F. Mukhanov and G. V. Chibisov, Pisma Zh. Eksp. Teor. Fiz. 33, 549 (1981) [JETP Lett. 33, 532 (1981)]; S. W. Hawking, Phys. Lett. B 115, 295 (1982); A. A. Starobinsky, Phys. Lett. B 117, 175 (1982); J. M. Bardeen, P. J. Steinhardt and M. S. Turner, Phys. Rev. D 28, 679 (1983).
  - [20] E. Komatsu et al. arXiv:1001.4538 [astro-ph.CO]; B. Gold et al., arXiv: 1001.4555 [astro-ph.GA]; D. Larson et al., arXiv: 1001.4635 [astro-ph.CO].
  - [21] G. Belanger, A. Belyaev, M. Brown, M. Kakizaki and A. Pukhov, Phys. Rev. D87, 016008 (2013).
  - [22] P. Ade et al. (Planck Collaboration), Astron. Astrophys. 536, 16464 (2011); P. Ade et al. astro-ph/0604069; URL <http://www.rssd.esa.int/index.php?project=Planck>.
  - [23] P. J. E. Peebles and B. Ratra, Rev. Mod. Phys. 75, 559 (2003).
  - [24] P. G. Ferreira and M. Joyce, Phys. Rev. D 58, 023503 (1998).
  - [25] Eds. M. Abramowitz and I. A. Stegun, Handbook of Mathematical Functions with Formulas, Graphs, and Mathematical Tables (Dover, 1972), 9th printing; G. Arfken, The incomplete gamma function and related functions, Mathematical Methods for Physicists, 3rd edn. (Academic Press, 1985).